DOI: 10.1007/s12541-014-0498-3

Performance Evaluation of a Coordinate Measuring Machine's Axis using a High-Frequency Repetition Mode of a Mode-Locked Fiber Laser

Narin Chanthawong[1,#], Satoru Takahashi[1], Kiyoshi Takamasu[1], and Hirokazu Matsumoto[1]

1 Department of Precision Engineering, The University of Tokyo, 7-3-1 Hongo, Bunkyo-ku, Tokyo, 113-8656, Japan
Corresponding Author / E-mail: narin@nanolab.t.u-tokyo.ac.jp, TEL: +81-3-5841-26472, FAX: +81-3-5841-26472

KEYWORDS: Measurement, Mode-locked fiber laser, Fabry–Pérot etalon, CMM, Fiber-type interferometer

We developed a multi-Fabry-Pérot etalon (multi-FPE) for selecting high-frequency parts of repetition-frequency modes of a short-pulse mode-locked fiber laser at the wavelength of 1.55 mm. The 5-GHz repetition-modified laser beam is transmitted to a fiber-type Michelson interferometer. The interference fringes exhibit a temporal coherence pattern and can be used for measuring spatial positioning. The performance of CMM's axis was determined directly from different positions of two interference fringes.

Manuscript received: October 18, 2012 / Revised: January 26, 2014 / Accepted: January 26, 2014

NOMENCLATURE

c = speed of light in vacuum (299,792,458 m/s)
n = phase refractive index of air
a = number of different indices between two pulses
f = frequency
l_c = cavity length
R = reflectivity of mirrors used in the etalon
f_{rep} = repetition frequency of frequency comb
l_0 = length of the CMM [m]

1. Introduction

Recently, coordinate measuring machines (CMMs) have become important in a number of industrial fields due to their ability to measure three-dimensional artifacts with complex shapes. In practice, the performance of CMMs must be monitored otherwise it can affect the quality of the final product. Various methods for evaluating the performance of CMMs have been proposed.[1-3] ISO standard protocols describe measurement methods based on physical standards (gauge blocks, step gauges, ball plates, etc.) or laser interferometers.[4] Current laser interferometer systems are based on continuous He-Ne lasers and fringe counting. One restriction imposed by this method is that the measurement path cannot be interrupted during the measurement period.

Recent studies have shown that following the development of carrier-envelope-phase stabilized lasers, femtosecond mode-locked pulses can be used as a reliable rule for measurement in the fields of ultrashort pulse lasers.[5-7] The pulse train shows a discrete frequency spectrum in the form of regularly spaced lines known as a frequency comb. Frequency combs are used as a frequency standard when the frequency repetition and the carrier-envelope offset refer to an SI reference standard, such as an atomic clock. These unique properties allow frequency combs to be used for time and frequency metrology,[8,9] fundamental physics,[10,11] and high-precision spectroscopy.[12,13] Frequency combs can also be extended into the extreme ultraviolet (XUV) region for X-ray imaging and precision quantum electrodynamics (QED) tests.[14] In 2002, practical experiments were conducted using the high temporal coherence between a pair of pulse trains for measurement of the group refractive index of air.[15] The pulse-to-pulse phase relation of an optical frequency comb has created new directions for high-accuracy long-range distance measurement.[16-20]

The mode spacing of such combs is given by the pulse repetition rate, which depends on the laser type and is typically of the order of 100 MHz. While it may be possible to increase the repetition rate, it is an expensive procedure requiring extensive and highly specific knowledge for practical use. One alternative would be to use an

 Springer

external Fabry-Pérot etalon to generate multiple pulses.[21]

In this work, to avoid the difficulties associated with obstacles in the measurement path in the case of He-Ne lasers, we apply a femtosecond mode-locked pulse laser for CMM's axis performance verification and use the temporal coherence property of optical frequency combs for length standard measurements. The temporal coherence pattern is used as a precise rule. This idea can be used in practice, and we reported the idea of using optical frequency combs as a standard for distance measurement in 2011[22] and gauge block calibration in 2012.[23] To increase the repetition rate of the temporal coherence pattern, a Fabry-Pérot etalon (FPE) system is developed to increase the repetition rate of a mode-locked fiber laser. The 100-MHz repetition rate of the femtosecond mode-locked laser is transferred to a 5-GHz filter (the developed FPE), where the repetition rate is changed to 5 GHz by selecting every 50th harmonic frequency passed by the etalon. The uncertainty in the stability of the modified laser is of order of 10^{-9}, which is considerably lower than the targeted measurement uncertainty in typical CMM verification.[24]

2. Principle

In this section, we briefly review the general idea of time-resolved experiments using a pulse laser and an unbalanced-arm Michelson interferometer, as shown in Fig. 1. An optical pulse from the mode-locked laser is split into two beams by an optical beam splitter. The two beams are then recombined after passing through various optical delays. The spatial distance l_d between the pulses is derived as $l_d = c/nf_{rep}$. The interference fringe position between two pulses with different indices is observed when the path difference between two arms of the interferometer is equal to half of the distance l_d:

$$l_2 - l_1 = a \cdot \frac{l_d}{2} = \frac{ac}{2nf_{rep}} \tag{1}$$

The interference fringe position is inversely proportional to f_{rep}. A high repetition rate entails more accurate spatial positioning of the interference fringe. However, high-repetition-rate comb lasers are expensive and require extensive and specific knowledge for practical use.

As an alternative, we can increase the repetition rate by selecting only high-frequency parts of the repetition rate modes of a frequency comb laser. An FPE is developed for this purpose as an optical cavity in which a laser beam undergoes multiple reflections between two reflecting surfaces, and whose resulting optical transmission is periodic in the optical frequency spectrum. The spectral transmission function from an FPE can be calculated by

$$T(f, R, l_c) = \frac{(1-R)^2}{(1-R)^2 + 4R\sin^2(2\pi f l_c/c)} \tag{2}$$

With high-frequency selection, the free spectral range (FSR) is set to an integer multiple m of the laser repetition rate f_{rep} by adjusting the FPE length as $f_{rep} = c/2nl$. The filter cavity then transmits exactly every m-th mode, while the unwanted intermittent modes are largely suppressed. The new repetition rate f'_{rep} of the frequency comb laser becomes

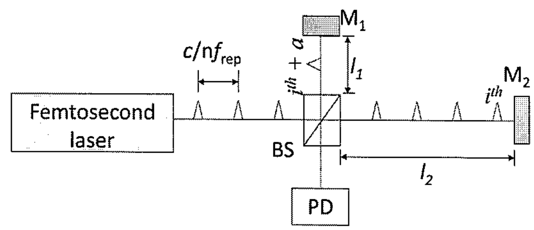

Fig. 1 Schematic setup of a time-resolved experiment using a femtosecond mode-locked pulse laser (frequency comb laser)

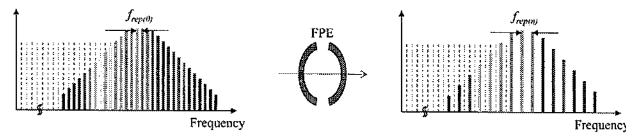

Fig. 2 Process of conversion the repetition rate

$$f'_{rep} = mf_{rep} \tag{3}$$

The transmission process of the repetition rate is shown in Fig. 2.

Therefore, half of the pulse distance ($l_d/2$) also changes as follows due to the new repetition rate:

$$a \cdot \frac{l_d}{2} = \frac{ac}{2nmf_{rep}} \tag{4}$$

which translates into more reference positions in space and can be changed by adjusting the FPE. A new repetition rate can be selected to create an appropriate reference fringe position for a CMM.

3. Fabry-Pérot Etalon

Two types of etalons are used in this study, a mirror FPE and a fiber FPE. Both types of low-finesse FPE are applied in series instead of a single high-finesse FPE to generate a repetition-modified laser pulse.

3.1 Fiber Fabry-Pérot etalon

The mirror-type FPE has the advantage of flexibility in terms of adjustable free spectral length, but a highly skillful operator and considerable amounts of time are required for mirror alignment. The idea of fiber FPEs was proposed to compensate for the disadvantages of mirror FPEs. Fig. 2 shows a single-mode fiber (SMF-28) cut to a specific length for creating a 1-GHz FSR. Both ends of the fiber are FC connectors whose surface is covered with a coating with 93% reflectivity. The length of the fiber FPE is checked by a tandem low-coherence interferometer with a high-precision translation stage (Sigmatech FS-3150PX, 10 nm resolution) attached to scan interference fringes. The measurement setup using a tandem low-coherence interferometer is shown in Fig. 3.

The system in Fig. 3 emits a light beam generated by a low-coherence light source. The low-coherence beam is confined to a single-mode fiber, which is connected to the fiber FPE. After passing through the FPE, the beam is conducted to a collimator (C_1) used for

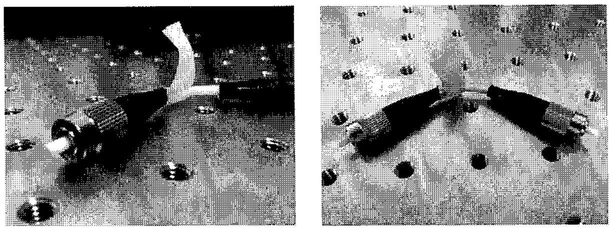

Fig. 3 A 1-GHz fiber FPE with coating with a 93% reflectivity at both ends

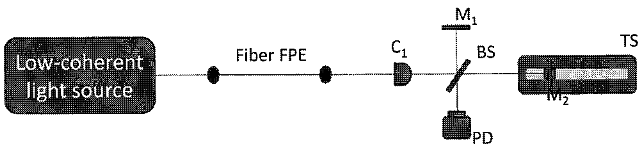

Fig. 4 A tandem low-coherence interferometer on a high-precision translation stage

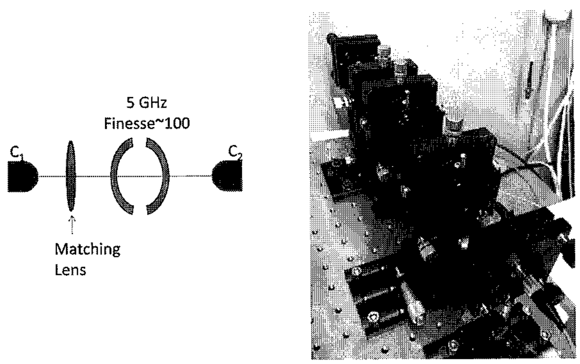

(a) (b)

Fig. 5 (a) Schematic diagram of concave mirror FPE. (b) A real picture of the FPE

the interferometer and split by a beam splitter (BS) into a reference-path beam with a fixed mirror (M_1) and a measurement-path beam where a mirror (M_2) is attached to a translation stage (TS; Sigmatech FS-3150PX, 10 nm resolution). Then the two beams are recombined in an InGaAs photodetector (PD; Newfocus 2011-FC) and the temporal interference fringes are observed.

3.2 Mirror Fabry-Pérot etalon

An FPE of the concave mirror type was selected for this experiment. A pair of concave mirrors with a radius of 300 mm, one inch diameter, a reflectivity of 97% and dielectric coating was used for the 5-GHz etalon setup. Visible-light laser alignment and a screen set at a distance of 2 m were used for parallel alignment of the FPE.

3.3 The FPEs system

The FPE system used in this study is a combination of a fiber FPE and a mirror FPE connected in series, as shown in Fig. 5, to increase the efficiency of the low-finesse etalons. A 100-MHz repetition fiber laser (MenloSystems C-fiber femtosecond laser, wavelength 1560 nm, output power 12 mW) with a repetition rate stabilized to a Rb

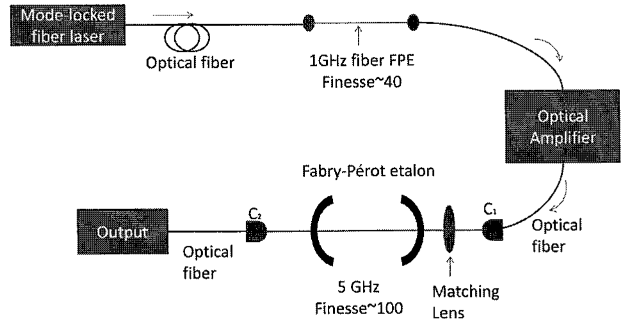

Fig. 6 Schematic diagram of the FPE system used

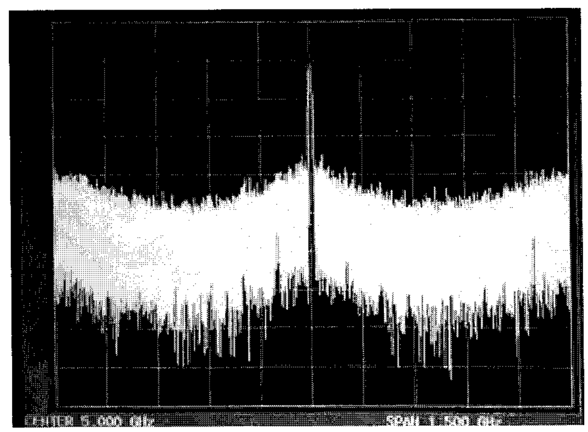

Fig. 7 Frequency spectrum of the beam after passing through the FPE

frequency standard (Stanford Research Systems FS725), was used as an optical pulse source. The laser beam was transmitted to the fiber etalon by a single-mode fiber optic cable. The repetition-modified laser was initially amplified using Erbium Doped Fiber Amplifier (EDFA) and subsequently applied to the mirror FPE through collimators (Thorlabs F810APC-1550, beam diameter 7.0 mm), and the output from the etalon was measured with a spectrum analyzer (Advantest R3265). The frequency spectrum is shown in Fig. 6.

After selecting the frequency mode of the etalon, the stability of the stability of the repetition rate of the frequency filtered comb was measured by beating with a 4.95-GHz frequency signal from a synthesized signal generator (Anritsu MG3632A). The Rb frequency was used as a reference for the synthesized signal. The beat signal was monitored for 2 hours with a universal counter (Iwatsu SC-7206, 0.1 Hz resolution) which was stabilized to the Rb frequency. The results of beating showed that the stability of the modified laser after passing through the FPE system was of the order of 10^{-9} over 2 hours, indicating that the repetition rate is sufficiently stable for length measurements.

4. Fiber-type Interferometer for CMM's Axis Verification

Fig. 6 shows the schematic setup for CMM's axis verification using a 5-GHz repetition mode of the mode-locked fiber laser. In this experiment, the interference fringe was created by 5-GHz repetition-modified laser at every 10 percents of the measuring range and it can

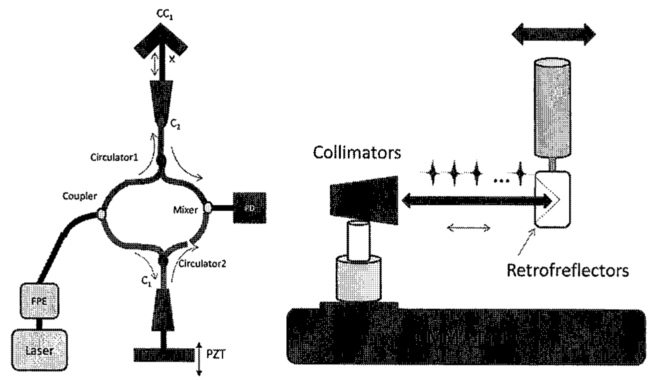

Fig. 8 Schematic setup for CMM evaluation using high-frequency repetitions of a mode-locked fiber laser

be increased by using higher repetition mode. The 5-GHz repetition-modified laser beam from the etalon was transmitted to a fiber-type interferometer, where the laser beam was split into two paths by a fiber coupler. One beam was used for the measurement path with a retro refractor attached to the CMM probe, and the other was used for the scanning path where a mirror was attached with an objective piezo positioner (PZT; Piezosystem Jena PX400) to scan the interference fringes. The beams from the two paths were combined by a fiber mixer. The distance between the interference fringes was determined with an InGaAs PD (Newfocus 2011-FC) in one-directional scanning of the reference mirror by PZT to avoid the creation of a hysteresis.

The experiment was performed on y-axis of a Mitutoyo Apex 707 CMM, starting by launching the laser beam to a 50/50 fiber coupler. The measurement path consisted of a fiber circulator and a collimator (C1), where the beam was reflected from a retro reflector and returned to the collimator. The reference path consisted of another set of a fiber circulator and collimator (C2), where the beam was reflected from a mirror attached to a PZT and returned to the collimator. The outputs from both circulators were combined by a fiber mixer and detected by the PD. Measurements can be performed in 5-GHz repetitions for every 30 mm of the CMM movement base.

5. Results

5.1 Measurement results

The experiment was performed in a room where temperature, pressure, and humidity were controlled and monitored during the experiment. The updated Edlén equation, in association with the actual environmental conditions, was used to compensate for the refractive index of air.[25] The measurement results corrected for the refractive index of air at the reference temperature are shown in Table 1.[26] The standard deviation of the measurement is about 0.1 mm. The measurement results imply that the repetition transformation technique can be used successfully for highly accurate measurements.

5.2 Uncertainty evaluation

In accordance with the ISO-recommended guidelines,[27] the overall uncertainty was evaluated for the CMM verification performed in this study. The sources of uncertainty are evaluated from related sources (measurement system, method, environment etc.) and shown in Table 2. One uncertainty is associated with laser stability at $2.89\times10^{-9}\cdot L_0$. Other sources related to the laser, such as repetition rate and carrier offset frequency, are smaller and negligible because the accuracy ratio with respect to the CMM is more than 100 times greater. The uncertainty for the refractive index of air is calculated to be $1.63\times10^{-8}\cdot L_0$ from the measurement errors associated with air temperature (0.001°C), pressure (10 mmHg), and humidity (1%RH), together with the uncertainty associated with the updated Edlen equation. The uncertainty related to the PZT, including PZT linearity and hysteresis, is 23.9 nm. Furthermore, the repeatability of measurement is found to be 50 nm, and the CMM resolution is evaluated to be 28.9 nm. The

Table 1 Experimental results for a 300-mm CMM's axis performance verification

CMM length (mm)	Comb length (mm)	Difference (m)
0.0000	0.0000	0.0
29.9713	29.9729	1.6
59.9426	59.9414	-1.2
89.9139	89.9164	2.5
119.8851	119.8852	0.1
149.8564	149.8542	-2.3
179.8277	179.8278	0.1
209.7990	209.8002	1.2
239.7703	239.7689	-1.4
269.7416	269.7431	1.5
299.7129	299.7123	-0.6

Table 2 Uncertainty evaluation in CMM performance verification

Sources of uncertainty	Uncertainty	Value (nm) for L_0= 300 mm
FPE modified pulse Laser	$2.89\times10^{-9}\cdot L_0$	0.43
Refractive index of air	$1.63\times10^{-8}\cdot L_0$	4.89
PZT	40 nm	23.9
Repeatability	100 nm	50
CMM Resolution	100 nm	28.9
System alignment	$1.3\times10^{-7}\cdot L_0$	39
Wave-front error	20 nm	11.6
Thermal expansion compensation	$5.77\times10^{-7}\cdot L_0$	173.2
Combined standard uncertainty (k=1)	$\sqrt{(63\text{mm})^2+(5.92\times10^{-7}\cdot L_0)^2}$	189

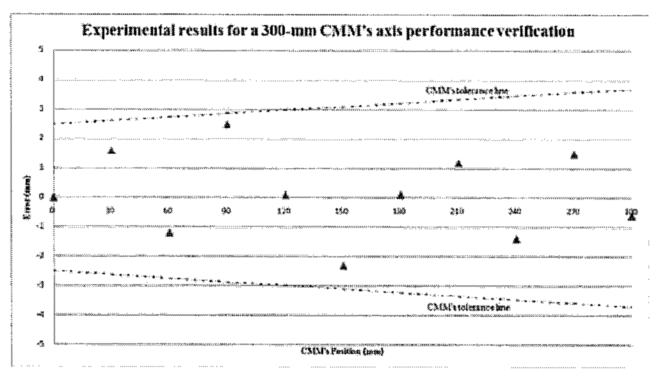

Fig. 9 The experimental results with CMM's tolerance limit

system alignment produces a further uncertainty of $1.3\times10^{-7}\cdot L_0$. The wave-front error is estimated at 11.6 nm. Finally, the uncertainty associated with the thermal expansion of the CMM is estimated at $5.77\times10^{-7}\cdot L_0$. Overall, the combined standard uncertainty is calculated to be 189 nm (k=1).

6. Conclusions

A new design for CMM performance verification by using temporal coherence of optical frequency combs was studied. A mode-locked fiber laser was stabilized to the frequency of a Rb clock (frequency standard). An FPE system combining a fiber FPE and a mirror FPE were connected in series to increase the repetition rate of a mode-locked fiber laser by selecting every 50th mode of the optical frequency comb. The stability over 2 hours showed that the modified optical comb is sufficiently stable to be used as a standard for CMM. The absolute length was determined from the half pulse interval distance of the FPE-modified pulse laser, and the performance of CMM was determined from interference fringes. The proposed measurement system based on a fiber-type interferometer is more convenient for CMM performance verification than currently adopted systems.

ACKNOWLEDGEMENTS

This research was financially supported under the Development of System and Technology for Advanced Measurement and Analysis Industrial Innovation Program of the Japan Science and Technology Agency (JST). Mr. Narin thanks the Royal Thai Scholarship for the scholarship provided.

REFERENCES

1. Umetsu, K., Furutnani, R., Osawa, S., Takatsuji, T., and Kurosawa, T., "Geometric Calibration of a Coordinate Measuring Machine using a Laser Tracking System, Measurement Science and Technology, Vol. 16, No. 12, pp. 2466-2472, 2005.
2. Weckenmann, A. and Lorz, J., "Monitoring Coordinate Measuring Machines by Calibrated Parts, Journal of Physics: Conference Series, Vol. 13, pp. 190-193, 2005.
3. Lee, S. J. and Chang, D. Y., 1-D Space Ball Array Calibration Methodology for Coordinate Measurement Machine, Journal of Physics : Conference Series, Vol. 13, pp. 194-197, 2005.
4. ISO 10360-2, "Geometrical Product Specifications (GPS) -- Acceptance and Reverification Tests for Coordinate Measuring Machines (CMM) -- Part 2: CMMs used for Measuring Linear Dimensions, 2009.
5. Jones, D. J., Diddams, S. A., Ranka, J. K., Stentz, A., Windeler, R. S., and et al., "Carrier-Envelope Phase Control of Femtosecond Mode-Locked Lasers and Direct Optical Frequency Synthesis, Science, Vol. 288, No. 5466, pp. 635-639, 2000.
6. Holzwarth, R., Udem, T., Hänsch, T. W., Knight, J., Wadsworth, W., and Russell, P. S. J., "Optical Frequency Synthesizer for Precision Spectroscopy, Physical Review Letters, Vol. 85, No. 11, pp. 2264-2267, 2000.
7. Cundiff, S. T. and Ye, J., "Colloquium: Femtosecond optical Frequency Combs, Reviews of Modern Physics, Vol. 75, No. 1, pp. 325-342, 2003.
8. Diddams, S. A., Bergquist, J. C., Jefferts, S. R., and Oates, C. W., "Standards of Time and Frequency at the Outset of the 21st Century, Science, Vol. 306, No. 5700, pp. 1318-1324, 2004.
9. Udem, T., Holzwarth, R., and Hänsch, T. W., "Optical Frequency Metrology, Nature, Vol. 416, No. 6877, pp. 233-237, 2002.
10. Lamine, B., Fabre, C., and Treps, N., "Quantum Improvement of Time Transfer between Remote Clocks, Physical Review Letters, Vol. 101, No. 12, Paper No. 123601, 2008.
11. Menicucci, N. C., Flammia, S. T., and Pfister, O., "One-Way Quantum Computing in the Optical Frequency Comb, Physical Review Letters, Vol. 101, No. 13, Paper No. 130501, 2008.
12. Schiller, S., "Spectrometry with Frequency Combs, Optics Letters, Vol. 27, No. 9, pp. 766-768, 2002.
13. Mandon, J., Guelachvili, G., and Picqu, N., "Fourier Transform Spectroscopy with a Laser Frequency Comb, Nature Photonics, Vol. 3, No. 2, pp. 99-102, 2009.
14. Kandula, D. Z., Gohle, C., Pinkert, T. J., Ubachs, W., and Eikema, K. S., "Extreme Ultraviolet Frequency Comb Metrology, Physical Review Letters, Vol. 105, No. 6, Paper No. 063001, 2010.
15. Yamaoka, Y., Minoshima, K., and Matsumoto, H., "Direct Measurement of the Group Refractive Index of Air with Interferometry between Adjacent Femtosecond Pulses, Applied Optics, Vol. 41, No. 21, pp. 4318-4324, 2002.
16. Ye, J., "Absolute Measurement of a Long, Arbitrary Distance to less than an Optical Fringe, Optics letters, Vol. 29, No. 10, pp. 1153-1155, 2004.
17. Cui, M., Schouten, R., Bhattacharya, N., and Berg, S., "Experimental demonstration of Distance Measurement with a Femtosecond Frequency Comb Laser, Journal of the European Optical Society-Rapid publications, Vol. 3, Paper No. 08003, 2008.
18. Joo, K. N., Kim, Y., and Kim, S. W., "Distance Measurements by Combined Method based on a Femtosecond Pulse Laser, Optics Express, Vol. 16, No. 24, pp. 19799-19806, 2008.
19. Wei, D., Takahashi, S., Takamasu, K., and Matsumoto, H., "Analysis of the Temporal Coherence Function of a Femtosecond Optical Frequency Comb, Optics Express, Vol. 17, No. 9, pp. 7011-7018, 2009.
20. Zeitouny, M. G., Cui, M., Bhattacharya, N., Urbach, H. P., Van den Berg, S., and Janssen, A., "From a Discrete to a Continuous Model

for Interpulse Interference with a Frequency-Comb Laser, Physical Review A, Vol. 82, No. 2, Paper No. 023808, 2010.

21. Steinmetz, T., Wilken, T., Araujo-Hauck, C., Holzwarth, R., Hänsch, T., and Udem, T., "Fabry–Pérot Filter Cavities for Wide-Spaced Frequency Combs with Large Spectral Bandwidth, Applied Physics B, Vol. 96, No. 2-3, pp. 251-256, 2009.

22. Chanthawong, N., Takahashi, S., Takamasu, K., and Matsumoto, H., "Absolute Distance Measurement using High-Frequency Repetition Modes of a Mode-Locked Fiber Laser, Proc. of Frontiers in Optics Laser Science, Poster No. JTuA52, 2010.

23. Chanthawong, N., Takahashi, S., Takamasu, K., and Matsumoto, H., "A New Method for High-Accuracy Gauge Block Measurement using 2 GHz Repetition Mode of a Mode-Locked Fiber Laser, Measurement Science and Technology, Vol. 23, No. 5, Paper No. 054003, 2012.

24. ISO 10012, "Measurement Management Systems -- Requirements for Measurement Processes and Measuring Equipment, 2003.

25. Birch, K. and Downs, M., "An Updated Edlén Equation for the Refractive Index of Air, Metrologia, Vol. 30, No. 3, pp. 155-162, 1993.

26. ISO 1, "Geometrical Product Specifications (GPS) -- Standard Reference Temperature for Geometrical Product Specification and Verification, 2002.

27. BIPM, "JCGM 100:2008 Evaluation of Measurement Data-Guide to the Expression of Uncertainty in Measurement," http://www.bipm.org/utils/common/documents/jcgm/JCGM_100_2008_E.pdf (Accessed 15 JUL 2014)